

# Role of isoconversional methods in varying activation energies of solid-state kinetics

## I. isothermal kinetic studies

Ammar Khawam\*, Douglas R. Flanagan

Division of Pharmaceutics, College of Pharmacy, University of Iowa, 115 S. Grand Av., Iowa City, IA 52242, USA

Received 6 October 2004; received in revised form 24 November 2004; accepted 29 November 2004

Available online 4 January 2005

### Abstract

Solid-state kinetics was developed from kinetic concepts for reactions in homogeneous phase systems, which has created considerable debate over issues such as variable activation energy. This behavior has been viewed by some as a violation of basic chemical kinetic principles. Variation in activation energy has been detected by isoconversional or ‘model-free’ calculation methods. The relationship between different calculation methods and the occurrence of variable activation energy was investigated in this work by employing model-fitting and isoconversional methods to analyze simulated isothermal data. In addition, these approaches were applied for sulfameter–dioxolane solvate desolvation data. We showed that variable activation energy is of two types—a true variation that results from the complex nature of the solid-state process and an artifactual one resulting from the use of some isoconversional methods.

© 2004 Elsevier B.V. All rights reserved.

**Keywords:** Solid-state kinetics; Isothermal kinetics; Activation energy; Arrhenius equation; Desolvation; Sulfameter; Isoconversion

### 1. Introduction

Solid-state kinetic studies have caused numerous debates and controversies [1,2]. One controversial issue is the variation of activation energy as a function of reaction progress. In a recent article, Galwey [3] questioned the meaning of variable activation energy in solid-state decompositions and proposed several explanations for this observation. Vyazovkin [4], in reply, provided alternative explanations for this behavior. Most explanations focus on the complexities inherent in solid-state kinetics with little consideration being given to secondary effects such as the effects of mathematical or computational methods. The aim of this work is to test the sensitivity of some of these methods, which will be done through kinetic analysis of simulated isothermal data, in addition to actual experimental kinetic results.

#### 1.1. Rate laws and kinetic analysis

The rate of a solid-state degradation reaction can be generally described by

$$\frac{d\alpha}{dt} = kf(\alpha) \quad (1)$$

where  $k$  is the reaction rate constant,  $f(\alpha)$  the reaction model and  $\alpha$  the conversion fraction. Integrating the above equation gives the integral rate law

$$g(\alpha) = kt \quad (2)$$

where  $g(\alpha)$  is the integral reaction model. The temperature dependence of the rate constant is usually described by the Arrhenius equation [5]:

$$k = A e^{-E_a/RT} \quad (3)$$

where  $A$  is the pre-exponential (frequency) factor,  $E_a$  the activation energy,  $T$  the absolute temperature and  $R$  the gas

\* Corresponding author. Tel.: +1 319 335 8819; fax: +1 319 335 9349.  
E-mail address: [ammar-khawam@uiowa.edu](mailto:ammar-khawam@uiowa.edu) (A. Khawam).

Table 1  
Solid-state rate expressions for different reaction models

Model	Differential form $f(\alpha) = (1/k)(d\alpha/dt)$	Integral form $g(\alpha) = kt$
Nucleation models		
Power law (P2)	$2\alpha^{1/2}$	$\alpha^{1/2}$
Power law (P3)	$3\alpha^{2/3}$	$\alpha^{1/3}$
Power law (P4)	$4\alpha^{3/4}$	$\alpha^{1/4}$
Avrami–Erofe'ev (A2)	$2(1-\alpha)[- \ln(1-\alpha)]^{1/2}$	$[- \ln(1-\alpha)]^{1/2}$
Avrami–Erofe'ev (A3)	$3(1-\alpha)[- \ln(1-\alpha)]^{2/3}$	$[- \ln(1-\alpha)]^{1/3}$
Avrami–Erofe'ev (A4)	$4(1-\alpha)[- \ln(1-\alpha)]^{3/4}$	$[- \ln(1-\alpha)]^{1/4}$
Geometrical contraction models		
Contracting area (R2)	$2(1-\alpha)^{1/2}$	$[1-(1-\alpha)^{1/2}]$
Contracting volume (R3)	$3(1-\alpha)^{2/3}$	$[1-(1-\alpha)^{1/3}]$
Diffusion models		
1 D diffusion (D1)	$\frac{1}{2\alpha}$	$\alpha^2$
2 D diffusion (D2)	$[- \ln(1-\alpha)]^{-1}$	$[(1-\alpha)\ln(1-\alpha)] + \alpha$
3 D diffusion-Jander equation (D3)	$3(1-\alpha)^{2/3}/2(1-(1-\alpha)^{1/3})$	$[1-(1-\alpha)^{1/3}]^2$
Ginstling–Brounshtein (D4)	$(\frac{3}{2}((1-\alpha)^{-1/3} - 1))$	$1 - (2\alpha/3) - (1-\alpha)^{2/3}$
Reaction-order models		
Zero-order (F0)	1	$\alpha$
First-order (F1)	$(1-\alpha)$	$-\ln(1-\alpha)$
Second-order (F2)	$(1-\alpha)^2$	$(1-\alpha)^{-1} - 1$
Third-order (F3)	$(1-\alpha)^3$	$0.5 [(1-\alpha)^{-2} - 1]$

constant. Substituting Eq. (3) in the above two rate expressions gives

$$\frac{d\alpha}{dt} = A e^{-E_a/RT} f(\alpha) \quad (4)$$

and

$$g(\alpha) = A e^{-E_a/RT} t \quad (5)$$

Several reaction models [6] are listed in Table 1.

Kinetic parameters can be obtained from isothermal kinetic data by applying these rate laws with traditional model-fitting methods or with isoconversional (model-free) methods. Model-fitting methods involve two fits: the first determines the model that best fits the data (Eq. (2)) while the second determines specific kinetic parameters such as the activation energy ( $E_a$ ) and frequency factor ( $A$ ) using the Arrhenius equation (Eq. (3)). On the other hand, isoconversional methods calculate  $E_a$  values at progressive degrees of conversion without any modelistic assumptions. The standard isoconversional method [7] is based on taking the natural logarithm of Eq. (5) giving,

$$-\ln t = \ln \left( \frac{A}{g(\alpha)} \right) - \frac{E_a}{RT} \quad (6)$$

A plot of  $-\ln t$  versus  $1/T$  at each  $\alpha$  yields  $E_a$  (from the slope) for that  $\alpha$  regardless of the model.

Friedman's [8] method is based on taking the natural logarithm of Eq. (4) giving

$$\ln \left( \frac{d\alpha}{dt} \right) = \ln(Af(\alpha)) - \frac{E_a}{RT} \quad (7)$$

A plot of  $\ln(d\alpha/dt)$  versus  $1/T$  at each  $\alpha$  yields  $E_a$  (from the slope) for that  $\alpha$  regardless of the model.

Vyazovkin developed an advanced isoconversional method (AIC) [9,10] that can be utilized for analyzing isothermal and non-isothermal data based on

$$\left| \sum_{i=1}^n \sum_{j \neq i}^n \frac{J(E_{a\alpha}, T_i(t_\alpha))}{J(E_{a\alpha}, T_j(t_\alpha))} \right| = \min \quad (8)$$

where

$$J(E_a, T(t)) = \int_{t_\alpha - \Delta\alpha}^{t_\alpha} e^{-E_a\alpha/RT_0} dt$$

where  $T_0$  is the isothermal temperature,  $\Delta\alpha = 1/m$  with  $m$  being the number of  $\alpha$  segments chosen for integration (20 in our work). The activation energy ( $E_a$ ) represents the value that minimizes (min) the above equation.

Isoconversional methods do not directly compute a frequency factor and therefore usually report activation energy values only. Vyazovkin [11] has suggested an indirect method that utilizes an artificial isokinetic relationship to calculate a frequency factor for isoconversional methods.

### 1.2. Varying activation energy

Solid-state kinetics was developed from reaction kinetics in homogeneous systems (i.e. gases and liquids). The Arrhenius equation (Eq. (3)) relates the rate constant of a simple one-step reaction to the temperature through the activation energy ( $E_a$ ) and pre-exponential factor ( $A$ ). It has been generally assumed that activation energy ( $E_a$ ) and frequency factor ( $A$ ) remain constant, however, it has been shown [12–14] that in solid-state reactions these kinetic parameters may vary with the progress of the reaction ( $\alpha$ ). This variation can be detected by isoconversional methods. While this variation

appears to be in conflict with basic chemical kinetic principles, in reality, it may not be. Such behavior may show that solid-state kinetics are more complex and/or multi-step compared to reactions in homogeneous phases. There are several proposed explanations for varying  $E_a$  with reaction progress. Vyazovkin [13] has shown this behavior in homogeneous phases. Possible explanations for such variation in solid-state reactions have been summarized by Galwey [3].

A variation in activation energy could be observed for both elementary and complex reactions. An elementary reaction could show variable activation energy during its progress due to the heterogeneous nature of the solid sample, which could cause a systematic change in reaction kinetics due to product formation, crystal defect formation, intra-crystalline strain or other similar effects. Solid-state reactivity of an elementary reaction could also be affected by experimental variables that could change the reaction kinetics by affecting heat or mass transfer at a reaction interface [3].

If two or more elementary steps, each having a unique activation energy, control the rate of product formation, the reaction is usually called a complex reaction [15]. In such a reaction, a change in the activation energy as the reaction progresses would be observed. This change will depend on the contribution of each elementary step, which gives an 'effective' activation energy that varies with reaction progress. Kinetic complexities are not limited to multiple chemical steps. They may also include physical processes (e.g. sublimation, localized melting, adsorption–desorption, diffusion of a gaseous product, particle size and morphology effects, etc.) that have different activation energies [3].

Isoconversional methods, use several TGA or DSC data sets for kinetic analysis. When performing isothermal experiments, care should be taken to ensure that every run is done under the same experimental conditions (i.e., sample weight, purge rate, sample size distribution, particle morphology, etc.) so that only the temperature varies for each run. Experimental variation can be minimized, but not totally removed. For example, sample mass may vary from one run to the next and affect a reaction because [16]:

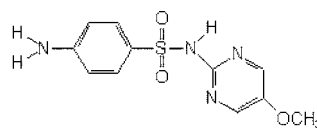
- a larger mass causes larger endothermic or exothermic effects (self-heating or self-cooling), producing deviations from the fixed temperature;
- the rate of diffusion of evolved gases through the sample will change with sample mass.

Similarly, sample packing could affect solid reaction kinetics where loosely packed powders contain air pockets that can reduce thermal conductivity or trap evolved gasses compared to a more densely packed powder. If any of the above effects occur, a thermogram can be altered such that it falls above or below the expected thermogram for isothermal studies. This could introduce errors in the calculation of kinetic parameters (i.e. activation energy) obtained from isoconversional methods.

We propose that the observed variation in activation energy as detected by isoconversional methods could be an ar-

tifact that results from the sensitivity of these methods to different experimental variables. This sensitivity was tested through kinetic analysis of simulated and actual experimental data. Actual experimental data was based on studying desolvation reaction kinetics of a drug solvate. A solvate crystal form is a form in which solvent molecules occupy specific positions within the crystal structure. Desolvation reactions are characterized by the removal of solvent molecules from the crystalline solvate below its melting point [17]. Such reaction kinetics can be studied by isothermal and non-isothermal thermal methods [18].

Sulfameter (structure below) is a long acting sulfonamide that is used for the treatment of urinary and respiratory tract infections [19]. A dioxolane (structure below) solvate of sulfameter was used to study desolvation reaction kinetics.



Sulfameter (5-methoxysulfadiazine)  
mw – 280.3



Dioxolane  
mw – 74.08

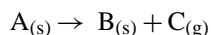
## 2. Experimental

There are two parts to this investigation: the first involves data simulation where several isothermal experiments were simulated and then analyzed mathematically and the second involved analyzing actual experimental data of the isothermal desolvation of sulfameter–dioxolane solvate.

The methods for evaluating isothermal kinetic data include the standard isoconversional method [7], Friedman's isoconversional method [8], Vyazovkin's advanced isoconversional (AIC) method [9,10] and the conventional model-fitting method.

### 2.1. Data simulation

A simple, one-step reaction (solid A producing solid B and gas C) according to the scheme below was simulated isothermally.



Fifteen simulations were generated using Microsoft® Excel from the integral form of the rate law (Eq. (5)), isothermal data was simulated by calculating the time ( $t$ ) for  $\alpha$  values between 0.01 and 0.99 according to:

$$t = \frac{g(\alpha)}{A e^{-E_a/RT}} \quad (9)$$

Values were assigned to the above parameters ( $g(\alpha)$ ,  $E_a$ ,  $A$  and  $T$ ) to calculate the time for each  $\alpha$ . In some simulations error was introduced to approximate variability encountered in real data. The generated kinetic data were then analyzed by different methods.

Table 2

Variations in isothermal simulations generated from simulation A1 (error-free), produced using a first-order reaction model (F1) with  $A = 1 \times 10^{15} \text{ min}^{-1}$  and  $E_a = 100 \text{ kJ/mole}$

Simulation	Simulation characteristics
A1	Error-free simulation of five isothermal curves at 323, 328, 333, 338 and 343 K
A2	323 K curve of simulation A1 shifted by $-10\%$ in time
A3	328 K curve of simulation A1 shifted by $-10\%$ in time
A4	333 K curve of simulation A1 shifted by $-10\%$ in time
A5	338 K curve of simulation A1 shifted by $-10\%$ in time
A6	343 K curve of simulation A1 shifted by $-10\%$ in time
A7	Temperature of 343 K curve in simulation A1 taken as 340 K
A8	Temperature of 333 and 343 K curves in simulation A1 taken as 335 and 340 K, respectively
A9	343 K curve of simulation A1 shifted by $-0.016 \text{ min}$
A10	343 K curve of simulation A1 shifted by $+0.016 \text{ min}$
A11	333 K curve of simulation A1 shifted by $-0.1 \text{ min}$
A12	333 K curve of simulation A1 shifted by $+0.1 \text{ min}$
A13	333 and 343 K curves of simulation A1 shifted by $+0.2$ and $-0.1 \text{ min}$ , respectively
A14	Simulations A7 and A9 combined
A15	0.5% random error in time introduced to each curve in simulation A1

The first isothermal simulation (A1) consisted of five isothermal ( $\alpha$ - $t$ ) curves which were simulated (error-free) at five temperatures (323, 328, 333, 338 and 343 K) using a first-order model ( $g(\alpha) = -\ln(1 - \alpha)$ ) with  $A = 1 \times 10^{15} \text{ min}^{-1}$  and  $E_a = 100 \text{ kJ/mole}$ . Fourteen additional simulations (A2–15) were generated from A1 using the same kinetic parameters and model but introducing different perturbations in each (Table 2). These perturbations included shifting one or more curves and/or changing the temperature of a curve. A curve shift simulates a thermal lag in a sample, while a temperature change simulates possible self-cooling/-heating effects or the effect of using an apparent sample temperature rather than the true temperature.

Kinetic analysis of each simulation was done by the conventional model-fitting method and several isoconversional methods (i.e. standard method [7], Friedman's method [8] and the advanced isoconversional method, AIC [9,10]).

All kinetic analysis was done with Microsoft Excel<sup>®</sup> using the Solver<sup>®</sup> tool for the AIC method or direct calculation for the standard and Friedman's methods. The differential ( $d\alpha/dt$ ) in Friedman's method was numerically evaluated without smoothing.

## 2.2. Sulfameter solvate desolvation

Sulfameter was obtained from Sigma<sup>®</sup> Chemical Co. (lot no. 107F0910) while dioxolane was obtained from Aldrich<sup>®</sup> Chemical Co. (lot no. LO14921KO). These chemicals were used as supplied. A dioxolane solvate of sulfameter was prepared by recrystallizing sulfameter from the neat solvent.

Desolvation kinetics of this solvate was followed isothermally by thermogravimetry using a Perkin-Elmer TGA 7. The TGA temperature was calibrated by a two-point calibra-

tion method using alumel and nickel. A flow of nitrogen gas ranging from 40 to 50 ml/min was used as a purge. A sample size of 3–5 mg was used for each kinetic run. Isothermal runs were performed at nominal temperatures of 323, 328, 333, 338 and 343 K; the exact sample temperature was obtained by averaging observed sample temperatures over the time of the TGA run.

Four different batches of sulfameter-dioxolane solvate were separately prepared, a sample from each batch was analyzed (samples 1–4). Samples 1 and 2 were run without controlling particle size or weight while samples 3 and 4 were sieved and a particle size range of 90–355  $\mu\text{m}$  was used and weights were within 5% of each other.

Kinetic analysis for desolvation data was done by model-fitting and isoconversional methods, as described earlier for simulated data.

## 3. Results and discussion

Thermogravimetric results of simulated and real data are shown in Figs. 1 and 2. Fig. 1 shows  $\alpha$  versus time plot for isothermal simulation (A1) which consists of five isothermal curves simulated (error-free) at five temperatures. Fig. 2 shows four isothermal desolvation thermograms for sulfameter-dioxolane samples (samples 1–4). Gravimetric weight loss for these solvates showed a 1:1 drug-solvent ratio ( $\sim 21\%$ , w/w). Kinetic analysis for simulated and real data sets is described below.

### 3.1. Simulated data

#### 3.1.1. Isoconversional methods

Isoconversional analysis (Figs. 3–8) showed that changing the temperature in isothermal runs does not affect the shape (i.e. linearity or slope) of the isoconversional ( $E_a$ - $\alpha$ ) plot. However, it does significantly change calculated  $E_a$  values, as seen in simulations A7 and 8 (Fig. 5). A change in the shape

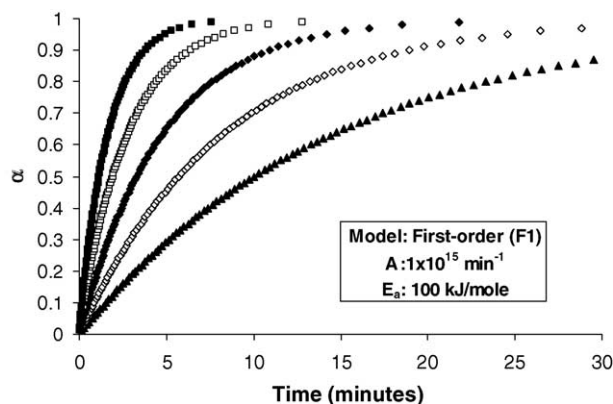


Fig. 1. Error-free simulation (A1) of  $\alpha$  vs. time for several isothermal kinetic runs at: ( $\blacktriangle$ ) 323 K; ( $\diamond$ ) 328 K; ( $\blacklozenge$ ) 333 K; ( $\square$ ) 338 K; ( $\blacksquare$ ) 343 K. The inset gives the simulation model, pre-exponential factor ( $A$ ) and activation energy ( $E_a$ ).

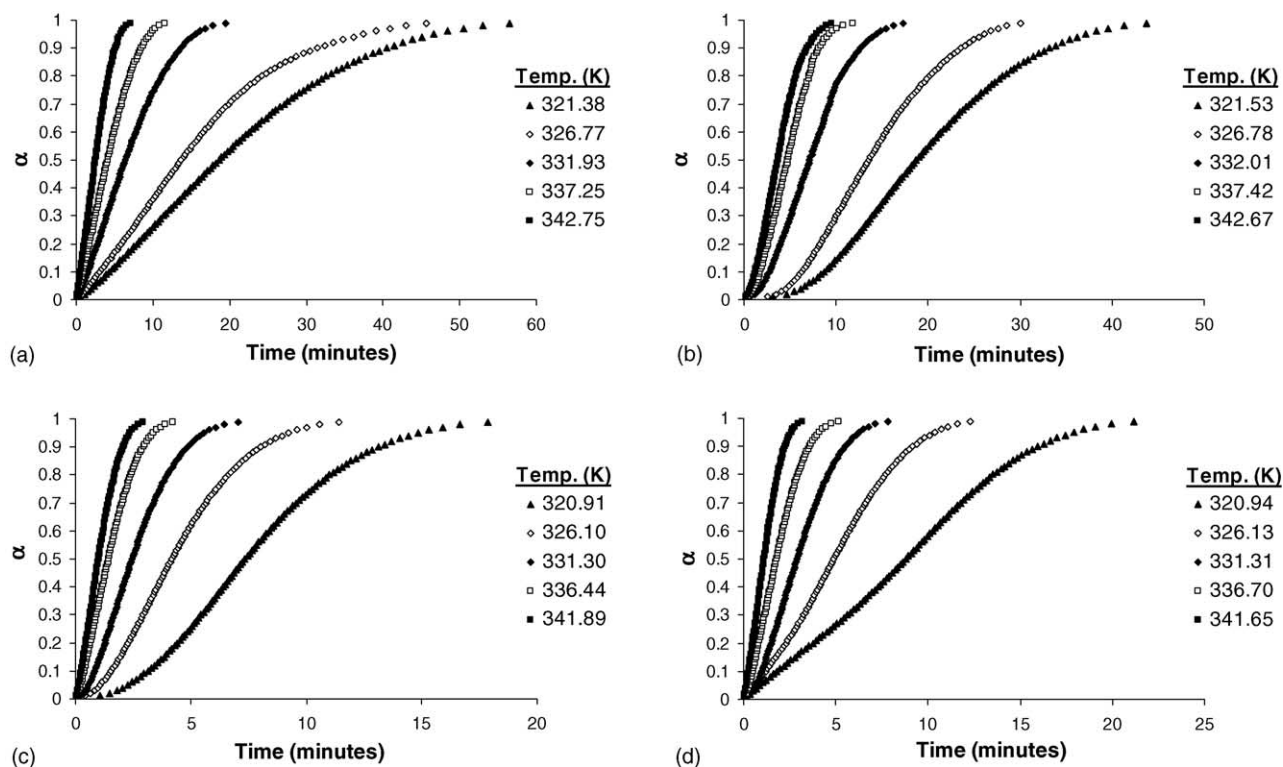


Fig. 2.  $\alpha$  vs. time plots for the isothermal desolvation of sulfamer–dioxolane solvate samples: (a) sample 1; (b) sample 2; (c) sample 3; (d) sample 4.

of an isoconversional plot represents an artificial variation in activation energy.

Shifting one or more curves had different effects based on the type of curve shift introduced. Systematic curve shifts (moving a curve by a constant percent (A2–6)) had no effect on the shape of the isoconversional plot, but considerably altered calculated values of  $E_a$  from all three isoconversional calculation methods (Fig. 4). On the other hand, shifting a curve by a fixed time (A9–13) significantly changed the shape of isoconversional plots calculated from the standard isoconversional method while those calculated from the Friedman and AIC methods were unaffected (Figs. 5–7). Changes in the

shape of isoconversional plots (i.e. the artificial variation in activation energy), are due to variation of introduced errors at each  $\alpha$ , the highest error being at low  $\alpha$  values, which accounts for the observed deviation in  $E_a$  from 100 kJ/mole in some simulations. For example, A9 and 10 (Fig. 5) show opposite deviations in  $E_a$  values that result from a  $\pm 0.016$  min curve shift (Table 2), which occur up to  $\alpha = 0.5$ . A similar result is seen for A11–14 (Figs. 6 and 7) where larger  $E_a$  deviations are seen compared to A9 and 10 due to larger introduced curve shifts (Table 2). Traditionally, researchers [20] have suggested analyzing solid-state kinetics over selected conversion values (i.e. 0.1–0.9) because errors are

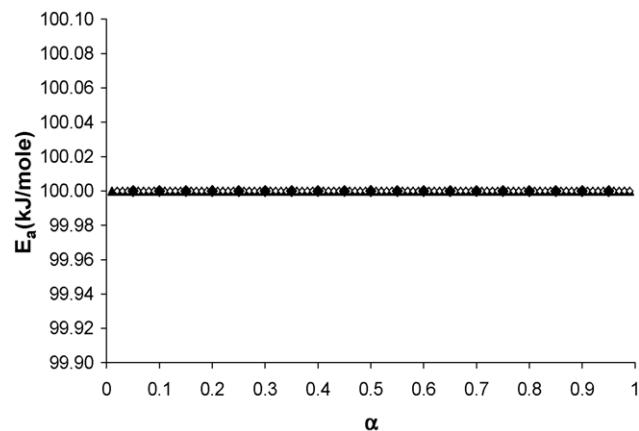


Fig. 3.  $E_a$  vs.  $\alpha$  plots of simulated isothermal runs (A1), evaluated by three isoconversional methods: (▲) standard; (◊) Friedman; (◆) AIC.

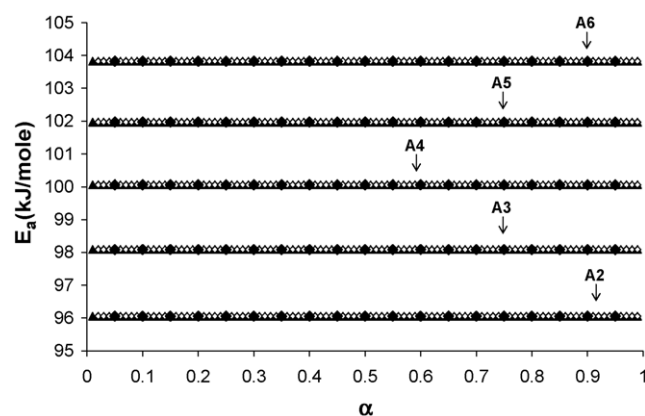


Fig. 4.  $E_a$  vs.  $\alpha$  plots of simulated isothermal runs (A2–6), evaluated by three isoconversional methods: (▲) standard; (◊) Friedman; (◆) AIC.

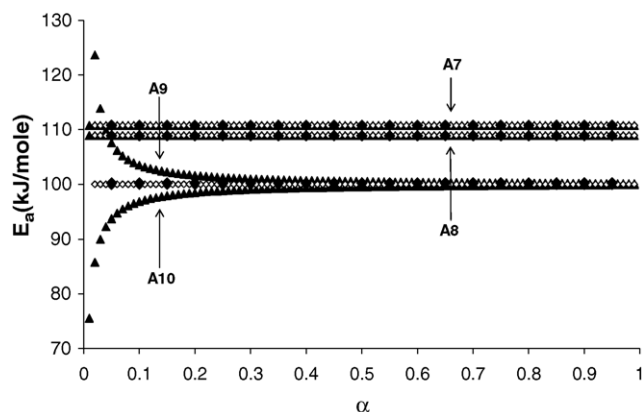


Fig. 5.  $E_a$  vs.  $\alpha$  plots of simulated isothermal runs (A7–10), evaluated by three isoconversional methods: ( $\blacktriangle$ ) standard; ( $\diamond$ ) Friedman; ( $\blacklozenge$ ) AIC.

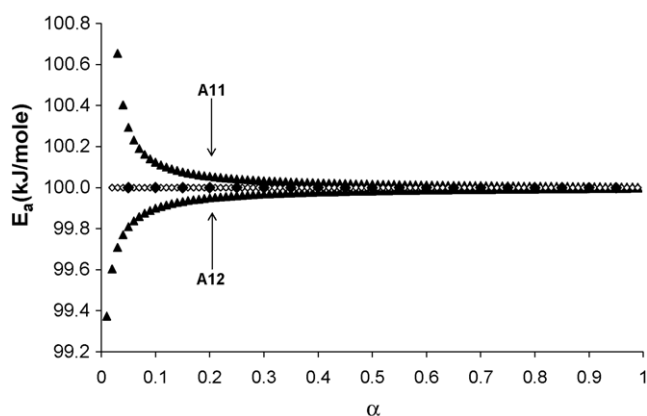


Fig. 6.  $E_a$  vs.  $\alpha$  plots of simulated isothermal runs (A11 and 12), evaluated by three isoconversional methods: ( $\blacktriangle$ ) standard; ( $\diamond$ ) Friedman; ( $\blacklozenge$ ) AIC.

usually highest at extreme conversion values (i.e.,  $\alpha < 0.1$  and  $\alpha > 0.9$ ).

Our results also show that some simulated runs were more sensitive to the same perturbation than others. Perturbations

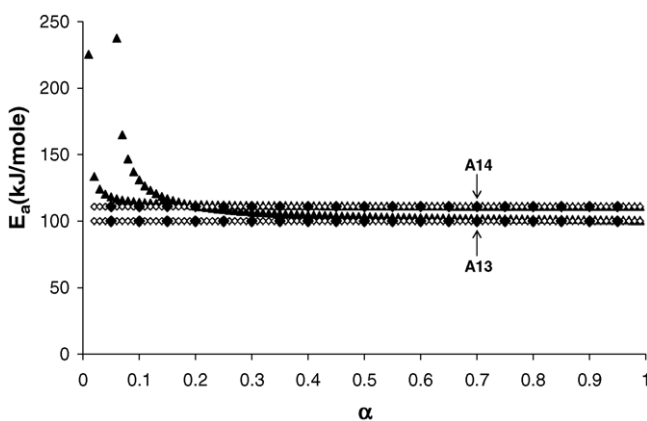


Fig. 7.  $E_a$  vs.  $\alpha$  plots of simulated isothermal runs (A13 and 14), evaluated by three isoconversional methods: ( $\blacktriangle$ ) standard; ( $\diamond$ ) Friedman; ( $\blacklozenge$ ) AIC.

affecting the middle curve (third of five) introduced less error than those affecting extreme curves (i.e. first or fifth curve). For example, when curves were systematically shifted by  $-10\%$  in A2–6 (Fig. 4), calculated values of  $E_a$  increased by about  $0.6\%$  in A4 where the third curve was shifted compared to a change of about  $4\%$  in A2 and A6 that involved shifting the first or last curve. Similarly, curves shifted by a fixed time as in A9–12 (Figs. 5 and 6) showed variable effects in the results calculated from the standard isoconversional method. For example, when the fifth curve (343 K curve) was shifted by  $\pm 0.016$  min as seen in A9 and 10 (Fig. 5), deviations in calculated  $E_a$  values as large as  $25\%$  were seen, however, when the curve shift was six times higher (curve shifted by  $\pm 0.1$  min) on the middle curve (333 K curve) as in A11 and 12 (Fig. 6), the deviation in calculated  $E_a$  values did not exceed  $0.6\%$ .

### 3.1.2. Model-fitting results

Kinetic analysis of each simulation was done by the conventional model-fitting method where several kinetic triplets (model,  $A$  and  $E_a$ ) were obtained (Table 3). Model selection (i.e. the first fit) was not affected by any introduced perturbation. The correct model (F1) was selected for all isothermal simulations (A1–15) and essentially perfect first-order plots were obtained ( $r = 1.000$ ). Model-fitting results agreed with those obtained from the Friedman and AIC methods, which showed that the model-fitting method is less sensitive to some of the perturbations (namely, curve shifts by a fixed time) compared to the standard isoconversional method. While the shape of the standard isoconversional plot changed for A9–13 (Figs. 5 and 7), kinetic parameters obtained by the model-fitting method for these simulations were not affected (Table 3). Both isoconversional and model-fitting results were similarly affected by either changing the isothermal temperature as in A7 and 8 (Fig. 5) or systematically shifting one or more curves as in A2–6 (Fig. 4).

Table 3

Fitted kinetic parameters for simulated isothermal data (Table 2) using model-fitting methods<sup>a</sup>

Simulation	$A$ ( $\text{min}^{-1}$ )	$E_a$ (kJ/mole)	$r^2$ <sup>b</sup>
A1	$1.00 \times 10^{15}$	100.00	1.0000
A2	$2.46 \times 10^{14}$	96.06	0.9984
A3	$5.12 \times 10^{14}$	98.09	0.9973
A4	$1.04 \times 10^{15}$	100.06	0.9970
A5	$2.08 \times 10^{15}$	101.97	0.9975
A6	$4.07 \times 10^{15}$	103.83	0.9986
A7	$5.23 \times 10^{16}$	110.77	0.9833
A8	$2.89 \times 10^{16}$	108.93	0.9650
A9	$1.00 \times 10^{15}$	100.00	1.0000
A10	$1.00 \times 10^{15}$	100.00	1.0000
A11	$1.00 \times 10^{15}$	100.00	1.0000
A12	$1.00 \times 10^{15}$	100.00	1.0000
A13	$1.02 \times 10^{15}$	100.06	1.0000
A14	$5.23 \times 10^{16}$	110.77	0.9833
A15	$9.85 \times 10^{14}$	99.96	1.0000

<sup>a</sup> Best fit model is always F1 (i.e., first-order).

<sup>b</sup> Correlation coefficient for  $\ln k$  vs.  $1/T$  plot.

### 3.2. Sulfameter desolvation

Kinetic analysis of sulfameter–dioxolane desolvation using the standard isoconversional method showed that shapes of isoconversional plots are substantially different. For the first two samples (Fig. 9a and b), this variation was anticipated since experimental variables were not as carefully controlled. However, for the second two samples (Fig. 9c and d), experimental conditions were nearly identical but the isoconversional plot still showed large differences at low conversion values, whereas at  $\alpha > 0.4$  both isoconversional plots obtained from the standard method are almost identical for these samples. This finding resembles results obtained for the same method for simulations A9 and 10 (Fig. 5) and A11 and 12 (Fig. 6).

Kinetic analysis done with the Friedman and advanced isoconversional (AIC) methods showed less variable activation energy compared to the standard isoconversional method (Fig. 10). However, calculated activation energies were highly scattered with the Friedman's method which was also seen in simulation A15 (Fig. 8) which is common with differential methods, the scatter could be reduced by smoothing but experimental information could be lost if this is not done carefully. There was also some scatter in the isothermal desolvation results obtained by the AIC method

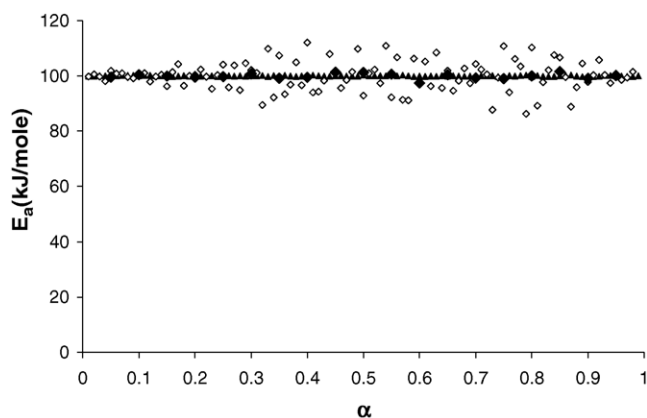


Fig. 8.  $E_a$  vs.  $\alpha$  plots of simulated isothermal runs (A15), evaluated by three isoconversional methods: (▲) standard; (◇) Friedman; (◆) AIC.

for both simulated (Fig. 8) and experimental data (Fig. 10), which can also be seen in some other AIC results [9]. This scatter is probably due to integration over small  $\alpha$  intervals.

Kinetic analysis done with the model-fitting method (Table 4) gave  $E_a$  values that agreed with those obtained from the AIC method. Results obtained from the model-fitting method also showed an agreement with those obtained from the standard isoconversional method for  $\alpha > 0.4$ .

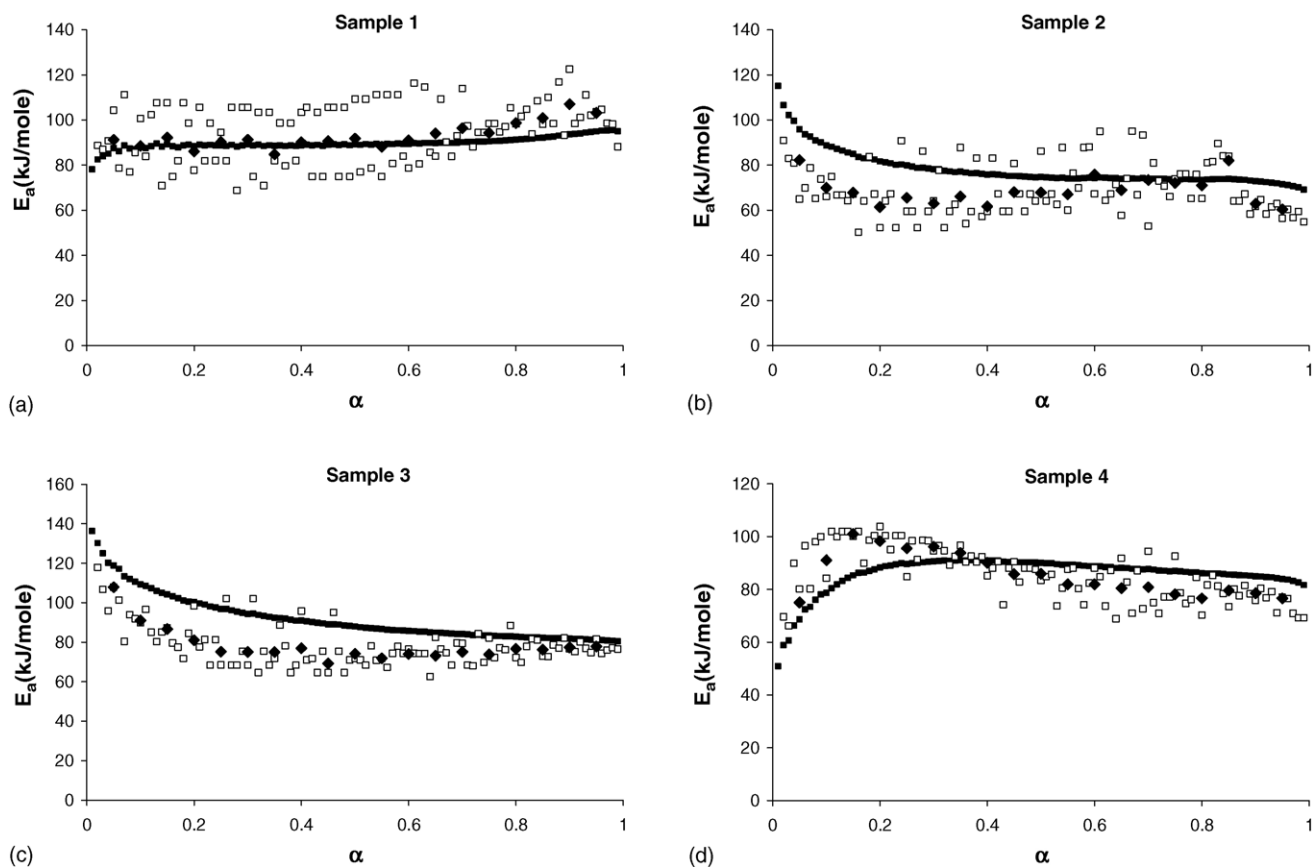


Fig. 9.  $E_a$  vs.  $\alpha$  plots for isothermal sulfameter–dioxolane solvate desolvation runs (samples 1–4), evaluated by three isoconversional methods: (■) standard; (□) Friedman; (◆) AIC.

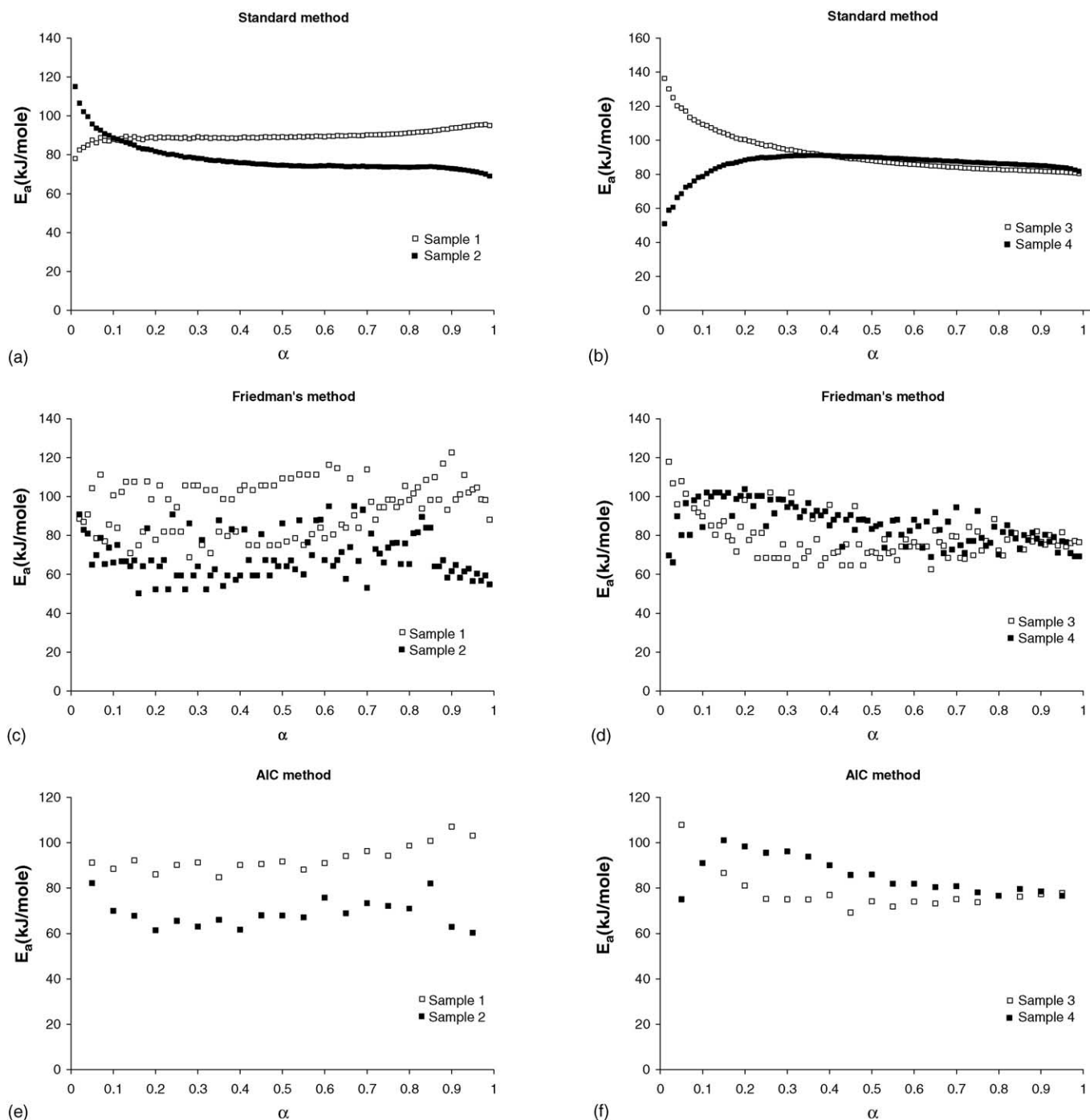


Fig. 10.  $E_a$  vs.  $\alpha$  plots for isothermal sulfameter-dioxolane solvate desolvation runs of four samples. Plots a, c and e are for samples 1 and 2. Plots b, d and f are for samples 3 and 4.

Model-fitting results also showed that calculated activation energies were not very dependent upon the kinetic model (Table 4). This means that for the same run, any model gives very comparable activation energies, which agrees with previous reports [21,22].

Comparison of activation energies obtained from different methods suggests that the observed variation in  $E_a$  in the standard isoconversional method for samples 3 and 4 is

artificial, which could be due to a less-controlled experimental variable that may have shifted any of the  $\alpha$ -time curves for these two samples (Fig. 2). These two samples gave widely varying  $E_a$  values up to  $\alpha \sim 0.4$ . It seems that desolvation of sulfameter-dioxolane solvate having a particle size of 90–355  $\mu\text{m}$  (samples 3 and 4) has an activation energy of 75–85 kJ/mole if the results of the standard method for  $\alpha > 0.4$  are to be believed, which agrees with the results



Table 4  
Fitted kinetic parameters for sulfamer–dioxolane isothermal desolvation kinetics by model-fitting methods

Model	Sample 1			Sample 2			Sample 3			Sample 4		
	$A$ ( $\text{min}^{-1}$ )	$E_a$ (kJ/mole)	$r$	$A$ ( $\text{min}^{-1}$ )	$E_a$ (kJ/mole)	$r$	$A$ ( $\text{min}^{-1}$ )	$E_a$ (kJ/mole)	$r$	$A$ ( $\text{min}^{-1}$ )	$E_a$ (kJ/mole)	$r$
A2	$6.89 \times 10^{13}$	94.61	0.9980	$5.26 \times 10^9$	67.90	0.9992 <sup>a</sup>	$2.67 \times 10^{11}$	75.91	0.9995 <sup>a</sup>	$5.12 \times 10^{12}$	84.55	0.9983 <sup>a</sup>
A3	$5.36 \times 10^{13}$	94.92	0.9890	$3.67 \times 10^9$	67.88	0.9954	$1.78 \times 10^{11}$	75.78	0.9915	$3.04 \times 10^{12}$	84.09	0.9943
A4	$4.39 \times 10^{13}$	95.07	0.9790	$2.84 \times 10^9$	67.88	0.9884	$1.34 \times 10^{11}$	75.70	0.9822	$2.17 \times 10^{12}$	83.86	0.9871
D1	$4.34 \times 10^{13}$	94.51	0.9879	$3.09 \times 10^9$	67.63	0.9805	$1.96 \times 10^{11}$	76.24	0.9846	$3.82 \times 10^{12}$	84.92	0.9818
D2	$3.13 \times 10^{13}$	94.04	0.9785	$2.71 \times 10^9$	67.70	0.9676	$1.67 \times 10^{11}$	76.23	0.9761	$3.98 \times 10^{12}$	85.49	0.9672
D3	$1.15 \times 10^{13}$	93.33	0.9275	$1.43 \times 10^9$	68.01	0.9136	$7.82 \times 10^{10}$	76.17	0.9278	$2.59 \times 10^{12}$	86.37	0.9103
D4	$8.13 \times 10^{12}$	93.80	0.9674	$7.88 \times 10^8$	67.79	0.9552	$4.71 \times 10^{10}$	76.22	0.9657	$1.25 \times 10^{12}$	85.78	0.9538
F1	$1.03 \times 10^{14}$	93.80	0.9666	$1.09 \times 10^{10}$	68.02	0.9576	$5.71 \times 10^{11}$	76.09	0.9675	$1.55 \times 10^{13}$	85.72	0.9554
F2	$4.56 \times 10^{14}$	92.11	0.6227	$1.46 \times 10^{11}$	69.39	0.6130	$4.45 \times 10^{12}$	75.92	0.6315	$3.18 \times 10^{14}$	88.29	0.6069
F3	$1.04 \times 10^{16}$	91.61	0.3870	$6.38 \times 10^{12}$	70.69	0.3821	$1.17 \times 10^{14}$	75.76	0.3981	$1.51 \times 10^{16}$	89.82	0.3772
P2	$4.91 \times 10^{13}$	95.67	0.9377	$2.52 \times 10^9$	67.81	0.9520	$1.19 \times 10^{11}$	75.66	0.9402	$1.49 \times 10^{12}$	83.08	0.9528
P3	$4.13 \times 10^{13}$	95.83	0.9125	$2.02 \times 10^9$	67.83	0.9310	$8.92 \times 10^{10}$	75.50	0.9167	$1.07 \times 10^{12}$	82.80	0.9307
P4	$3.50 \times 10^{13}$	95.91	0.8968	$1.67 \times 10^9$	67.84	0.9176	$7.10 \times 10^{10}$	75.40	0.9019	$8.37 \times 10^{11}$	82.66	0.9166
R1	$5.39 \times 10^{13}$	95.22	0.9783	$3.12 \times 10^9$	67.74	0.9825	$1.72 \times 10^{11}$	75.99	0.9774	$2.49 \times 10^{12}$	83.83	0.9846
R2	$3.56 \times 10^{13}$	94.61	0.9981 <sup>a</sup>	$2.60 \times 10^9$	67.78	0.9954	$1.47 \times 10^{11}$	76.07	0.9971	$2.75 \times 10^{12}$	84.65	0.9959
R3	$2.65 \times 10^{13}$	94.36	0.9962	$2.15 \times 10^9$	67.83	0.9913	$1.2 \times 10^{11}$	76.09	0.9955	$2.51 \times 10^{12}$	84.98	0.9909

<sup>a</sup> Best fit model.

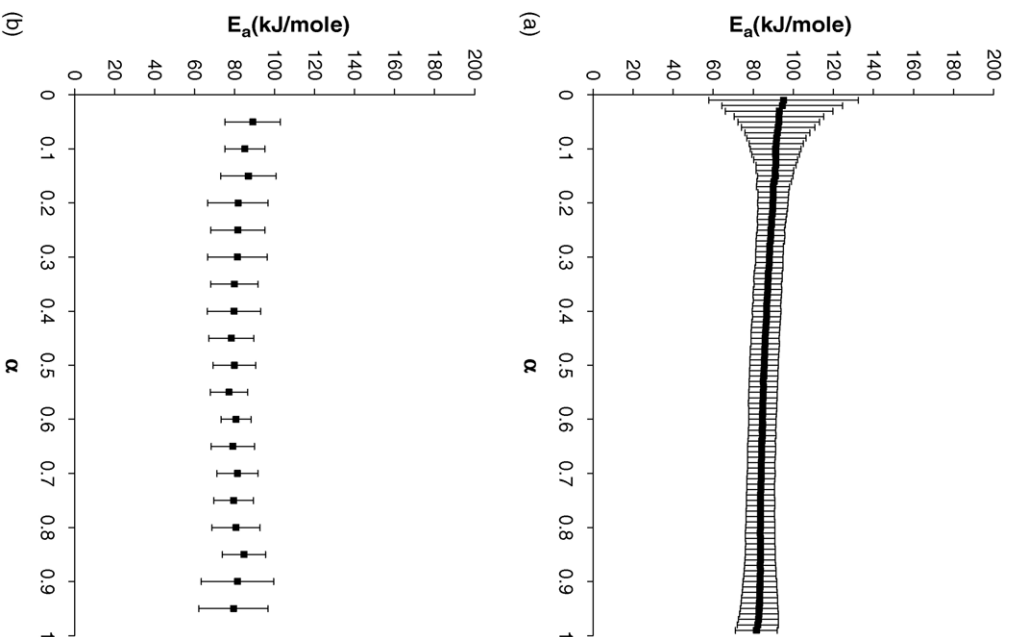


Fig. 11.  $E_a$  vs.  $\alpha$  plots for isothermal sulfamer–dioxolane solvate desolvation using the average of samples 1–4 with 95% confidence intervals, evaluated by the: (a) standard method; (b) AIC method.

obtained from the AIC (Fig. 9c and d) and model-fitting (Table 4) methods.

### 3.3. Confidence intervals for activation energies

To minimize experimental errors encountered, it is often necessary for experimental conditions to be rigorously controlled. For solid-state kinetic studies, this can be achieved by sieving the sample, using the same weight for each run ( $\pm 5\%$ ), controlling purge gas-flow rate as well as other variables. However, such variations cannot be totally eliminated and random experimental errors could produce significant variation in calculated kinetic parameters. Therefore, replicate samples should be analyzed, which permits calculating an average value of the activation energy with a confidence interval. The 95% confidence interval of the activation energy was calculated for the isothermal desolvation of sulfamer–dioxolane solvate (Fig. 11) by averaging all four previous runs (samples 1–4) even though two runs had less

well-controlled particle size and weights. For the standard isoconversional method (Fig. 11a), this average showed the widest confidence intervals ( $\pm 40\%$ ) for low  $\alpha$  ( $\alpha \leq 0.2$ ) while the smallest were  $\pm 8$ – $12\%$  for  $\alpha > 0.2$ . On the other hand, averaging all four runs for the AIC method (Fig. 11b) showed uniform confidence intervals of  $\pm 10$ – $20\%$  at all values of  $\alpha$ . Judging from the simulation results, plot (Fig. 11b) is probably more representative of the actual activation energy than that in (Fig. 11a).

The systematic decrease of confidence intervals with reaction progress seen in the standard isoconversional method further supports the somewhat artifactual activation energy variation at low  $\alpha$ .

#### 4. Conclusions

The debate over variable activation energy is most often due to viewing heterogeneous solid-state kinetics from a homogeneous perspective. However, explanations are necessary for this behavior to better understand solid-state reaction mechanisms.

Activation energy variation could be real or artifactual. A true variation in activation energy is one that occurs because of the inherent complexity of the solid sample, which includes different reactivity of individual particles due to particle size variations or crystal imperfections. Artifactual variations arise from the kinetic calculation methods employed. Our results showed the sensitivity of some calculation methods to introduced experimental variables. This sensitivity is manifested by an artifactual variation in activation energy as a function of  $\alpha$ . Methods do not equally contribute to the observed variation in activation energy. The standard isoconversional method gives the most activation energy variation, which does not occur with Friedman's or AIC methods. However, both methods show some data scattering, which is quite significant in Friedman's method such that it is far less useful for analyzing real experimental data if no data smoothing is employed.

The model-fitting method generates a single activation energy, which is both an advantage and a disadvantage. The advantage is that the frequency factor can be directly obtained and, like the Friedman and AIC methods, the activation energy is apparently least affected by experimental variables. The disadvantage is that this method cannot detect the complexity of some solid-state reactions as isoconversional methods can. Care should be taken when interpreting kinetic results from isoconversional methods, if the variation in activation energy is artifactual, this variation can lead to a

false mechanistic conclusion about a reaction being complex while, in fact, it is not.

The AIC method appears to be a superior isoconversional method and its use should be encouraged in isothermal experiments. The results from this method should be used in conjunction with those from the model-fitting method to determine the most accurate values of  $E_a$  and  $A$ . Finally, variation in activation energy could be a combination of the two aforementioned sources of variation, making the resolution into individual contributions difficult or impossible.

There seems to be no ideal method for evaluating solid-state kinetics because calculated values of activation energy could be in error, even when results from isoconversional and the model-fitting methods agree. To overcome this, experimental variables should be adequately controlled and experiments replicated, so that averaged kinetic parameters and their confidence intervals can be estimated.

Our next work involves similar simulations and experimental data for non-isothermal kinetic runs [23].

#### References

- [1] M.E. Brown, *J. Therm. Anal.* 49 (1997) 17.
- [2] A.K. Galwey, M.E. Brown, *J. Therm. Anal.* 60 (2000) 863.
- [3] A.K. Galwey, *Thermochim. Acta* 397 (2003) 249.
- [4] S. Vyazovkin, *Thermochim. Acta* 397 (2003) 269.
- [5] K.J. Laidler, *J. Chem. Educ.* 61 (1984) 494.
- [6] A.K. Galwey, M.E. Brown, *Thermal Decomposition of Ionic Solids: Chemical Properties and Reactivities of Ionic Crystalline Phases*, 1st ed., Elsevier, Amsterdam, 1999.
- [7] S. Vyazovkin, *Thermochim. Acta* 355 (2000) 155.
- [8] H.L. Friedman, *J. Polym. Sci., Part C: Polym. Lett.* 6 (1964) 183.
- [9] S. Vyazovkin, *J. Comput. Chem.* 22 (2001) 178.
- [10] S. Vyazovkin, *J. Comput. Chem.* 18 (1997) 393.
- [11] S. Vyazovkin, *Int. J. Chem. Kinet.* 28 (1996) 95.
- [12] S. Vyazovkin, C.A. Wight, *Annu. Rev. Phys. Chem.* 48 (1997) 125.
- [13] S. Vyazovkin, *New J. Chem.* 24 (2000) 913.
- [14] S. Vyazovkin, *Int. Rev. Phys. Chem.* 19 (2000) 45.
- [15] J.I. Steinfeld, J.S. Francisco, W.L. Hase, *Chemical Kinetics and Dynamics*, 2nd ed., Prentice-Hall, Upper Saddle River, NJ, 1999.
- [16] W.W. Wendlandt, *Thermal Analysis*, 3rd ed., Wiley, New York, 1986.
- [17] S.R. Byrn, R.R. Pfeiffer, J.G. Stowell, *Solid-State Chemistry of Drugs*, 2nd ed., SSCI Inc., West Lafayette, In., 1999.
- [18] M.E. Brown, *Introduction to Thermal Analysis: Techniques and Applications*, 2nd ed., Kluwer Academic Publishers, The Netherlands, 2001.
- [19] C.O. Wilson, O. Gisvold, R.F. Doerge, *Textbook of Organic Medicinal and Pharmaceutical Chemistry*, 8th ed., Lippincott, Philadelphia, 1982.
- [20] C.M. Wyandt, D.R. Flanagan, *Thermochim. Acta* 196 (1992) 379.
- [21] S. Vyazovkin, C.A. Wight, *Int. Rev. Phys. Chem.* 17 (1998) 407.
- [22] D.L. Zhou, D.J.W. Grant, *J. Phys. Chem. A* 108 (2004) 4239.
- [23] A. Khawam, D.R. Flanagan, *Thermochim. Acta*, in preparation.